Tuijin Jishu/Journal of Propulsion Technology
ISSN: 1001-4055
Vol. 44 No. 4 (2023)

Analytical Approximation of Corona Discharge and Dielectric Barrier Corona Discharge with Multi Points to Plane Configuration

[1]Muhammad Nur, [2]Asep Yoyo Wardaya, [3]Feni Musriah, [4]Belliany Dian Asmara Hadi, [5]Ketut Sofyan Firdausi, [6]Sumariyah

[2] [3] [4] [5] Physics Department, Faculty of Science and Mathematics, Diponegoro University, Tembalang Campus, Semarang 50275, Indonesia
[1] [2]Center for Plasma Research, Integrated laboratory, Universitas Diponegoro, Tembalang Campus, Semarang 50275, Indonesia

E-mail: sumariyah@lecturer.undip.ac.id, fajararianto@fisika.fsm.undip.ac.id

*Corresponding author Email: mnur@lecturer.undip.ac.id

Abstract: Electric field and current density produced by multi-point plane configurations to plane configuration of the corona plasma generators have been determined theoretically. The aims of this calculation are to determine the formulation of electric field and current density. The result shows that the plasma generator can produce an electric field whose value varies at different points around the electrode (nonuniform). The total electric field of the resulting from the superposition of the electric field vector of each point is only in the direction of z-axis due to the symmetry of the electric field vector. Current density value shows that the multi-points to plane electrode configuration produced saturated currents due to their asymmetric electrode. Other factors affecting the current density are the charge carrier mobility particle.
Keywords: electric field, current density, multi-points to plane configuration, corona discharge, dielectric barrier

1. Introduction

Corona discharge (CD) as a nonthermal atmospheric pressure plasma has been widely used to solve various problems such as reducing pollutant gases [1,2], waste water treatment [2], in biomedicine, bacterial decontamination and sterilization [3], sand surface modification [4]. Corona payload discharges have also been used in aviation. Corona discharges can remove unwanted electrical charges from the surface of a flying aircraft. This technique can avoid the negative impact of uncontrolled electrical discharges on avionics system performance. Corona discharge plasma is plasma that occurs in gas media due to the influence of a high electric field. This plasma can be generated using asymmetric electrode pairs [5,6]. Apart from that, CDs can also have a dielectric barrier added between the two electrodes. This type of discharge is often also known as a silent discharge. Dielectric barrier corona discharge (DBCD). Compared with parallel or coaxial plane geometries, the use of multipoint-to-plane geometries has several advantages, such as low operating voltage and low dielectric losses [4]. Studies of plasma electrical properties using multipoint-to-plane geometry have been carried out [7].

One of the physical problems that is important in corona discharge plasma is a plasma electrode configuration form for generating a high electric field and a large current density only by a small power [4]. In general, current density could be formed when the divergence of the electric field generated is not zero. This divergence value is largely determined by the asymmetry of the plasma electrode configuration as in the calculation of the field point configurations performed by Coelho and Debeau [8].

Calculation of electric field and current density have previously performed for a wide variety of configurations such as point-field which produces a large electric field around the end of the active electrode [8] and ring-plane configuration that do not generate current density because thin disk that is symmetrical radial cause the direction of the electric field that came out also radially symmetric [8].

This study aims to perform calculations of multi-points to plane configuration. Configuration model is expected to generate an electric field and current density as well as current and its validation This research also

examines the effect of the presence of a dielectric barrier (DBCD) on the characteristics of the current and voltage applied to a multi-point positive corona plasma reactor configuration.

2. Electric Field Equation Approach Hyperbole

Calculation of the electric field to the needle-plane configuration can be done using hyperbole coordinate approach as practiced by Coelho and Debeau [8]. Equations hyperbole for needle are written as [8]

$$x = c\sin\zeta\cosh\eta;$$
$$y = c\cos\zeta\sinh\eta, \qquad (1)$$

with parameter ζ and η are defined as hyperbolic coordinates [7]

$$\zeta = 0 \quad \text{on position} \quad (x = 0),$$
$$\zeta = \pi/2 \quad \text{on position} \quad (y = 0), \qquad (2)$$
$$\eta = 0 \quad \text{on position} \quad (y = 0).$$

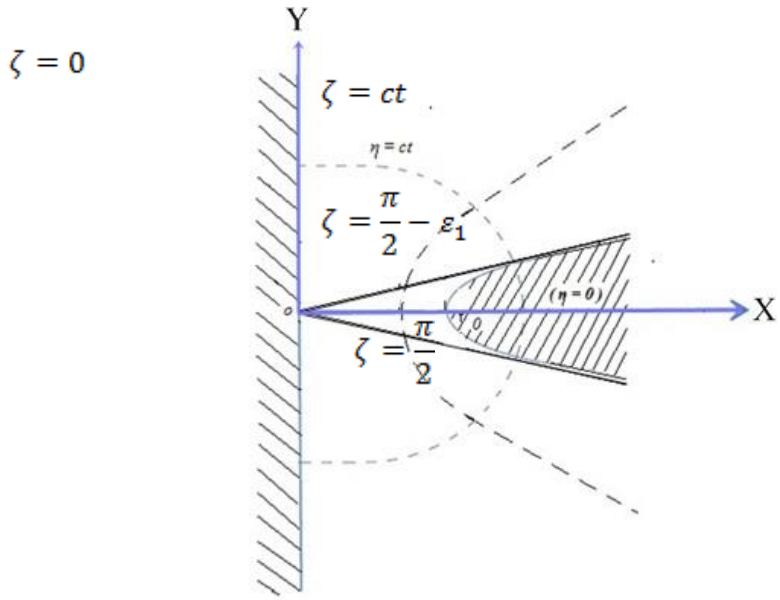

Fig 1: Representation of hyperbole-plane configuration [8]

The value of the electric field at a point can be obtained using the equation [8]

$$E(\zeta,\eta) = \frac{C}{c\cos\zeta\left(\cosh^2\eta - \sin^2\zeta\right)^{1/2}}, \qquad (3)$$

where

$$C = V\Big/\ln\left(\frac{2}{\varepsilon_1}\right). \qquad (4)$$

Equation (3) in the case of a needle electrode can be made into another formula using boundary conditions $\zeta = \frac{1}{2}\pi - \varepsilon_1$ where $\varepsilon_1 \ll 1$, which generates an electric field formula as [9]

$$E(\zeta,\eta)=\frac{\left[V/\ln\left(\frac{2}{\varepsilon_1}\right)\right]}{\sqrt{c^2\cos^4\zeta+y^2}}, \tag{5}$$

where [8]

$$\cos^2\zeta=\frac{u\pm\sqrt{u^2+4c^2y^2}}{2c^2}, \tag{6}$$

and u is defined as [8]

$$u=c^2-y^2-x^2=c^2\cos^2\zeta-\frac{y^2}{\cos^2\zeta}, \tag{7}$$

with [7]

$$\begin{aligned} x&=c\sin\zeta\cosh\eta;\\ y&=c\cos\zeta\sinh\eta. \end{aligned} \tag{8}$$

For the case of three dimensions with the same boundary conditions, equation (5) can be converted into

$$E(\zeta,\eta,\psi)=\frac{\left[V/\ln\left(\frac{2}{\varepsilon_1}\right)\right]}{\sqrt{c^2\cos^4\zeta+x^2+y^2}}, \tag{9}$$

where

$$\cos^2\zeta=\frac{u\pm\sqrt{u^2+4c^2\left(x^2+y^2\right)}}{2c^2}, \tag{10}$$

and u is defined as

$$u=c^2-\left(x^2+y^2+z^2\right)=c^2\cos^2\zeta-\frac{\left(x^2+y^2\right)}{\cos^2\zeta}, \tag{11}$$

with [8]

$$\begin{aligned} x&=-c\sinh\eta\cos\zeta\sin\psi;\\ y&=-c\sinh\eta\cos\zeta\cos\psi;\\ z&=c\cosh\eta\sin\zeta; \end{aligned} \tag{12}$$

with η, ζ, and ψ is 3-dimensional coordinates of hyperbole.

3. Gauss' Law and Divergence Theorem

Gauss' law states "The number of lines of force coming out of a closed surface is proportional to the amount of electric charge covered by the closed surface".

Law Gauss divergence theorem developed into the changing shape of the closed surface integral into a volume integral [10]. Mathematically this can be written as follows:

$$\psi=\oint\mathbf{E}\bullet d\mathbf{A}=\int\nabla\bullet\mathbf{E}\,d\sigma=\sum_i\frac{q_i}{\varepsilon_0}, \tag{13}$$

where the value of the divergence of the electric field is:

$$\nabla\bullet\mathbf{E}=\frac{q}{\varepsilon_0}. \tag{14}$$

With S is a closed surface, $\sum_i q_i$ is the amount of charge that is surrounded by a closed surface S, ψ is the potential difference, $d\boldsymbol{A}$ is the element of area A, $d\sigma$ is the element of volume σ and ε_0 is the permittivity of vacuum.

Capacitance

Capacitance is a quantitative measure the capacitance of the capacitor [9]. The value of capacitance elements on the element area is:

$$dC = \varepsilon_0 \frac{dA}{h}. \tag{15}$$

The relationship between capacitance and electric field can be calculated with Gauss's law,

$$\varepsilon_0 \oint \mathbf{E} \bullet d\mathbf{A} = q, \tag{16}$$

With the value $q = VC$, V is the input voltage and C is the capacitance value.

Current Density Equation

For the calculation of the current density on corona plasma generator, we use the formulation [11]:

$$\mathbf{j} = ne\mu\mathbf{E}, \tag{17}$$

where [10]

$$ne = \varepsilon\left(\nabla \bullet \mathbf{E}\right), \tag{18}$$

So that

$$\mathbf{j} = \mu\varepsilon\left(\nabla \bullet \mathbf{E}\right)\mathbf{E}, \tag{19}$$

the divergence $\mathbf{E}$ in Cartesian coordinates is written as:

$$\nabla = \frac{\partial}{\partial x}\mathbf{a}_x + \frac{\partial}{\partial y}\mathbf{a}_y + \frac{\partial}{\partial z}\mathbf{a}_z \tag{20}$$

4. Methods

4.1 Multi-Points to Plane Configuration Model

Multi-points to plane configuration model as shown in Figure 2, consists of two square plate with a side of *d* where there are five needles were stuck on one plate. The distance between the needle electrode is *a* and length of each needle is *b*. The distance from the tip of the needle electrode to the plate without the needle is *c*.

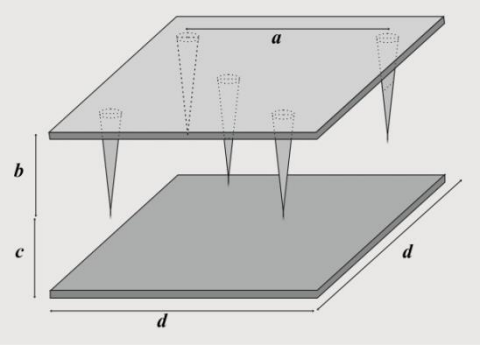

(a)

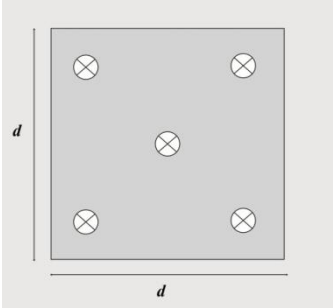

(b)

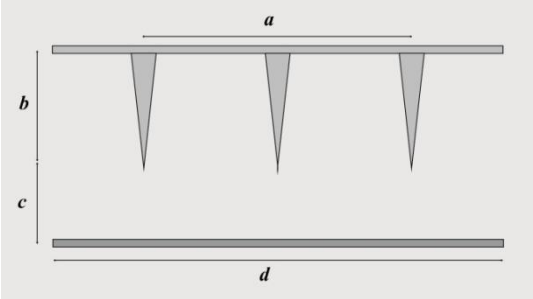

(c)

Fig 2: Corona discharge plasma generator with a multi-point to configuration with (a) representation multi-point electrode models in 3-dimensional (b) representation of the model when viewed from above the plate (c) representation of the model when viewed from the side

5. Results And Discussion

5.1 Electric Field of Multi-Points to Plane

The electric field at *a* distance from the tip of the needle electrode can be obtained by calculated the electric field that was generated by one needle at position 1 of Figure 3. Mark (X) in the figure indicates the position of the needle.

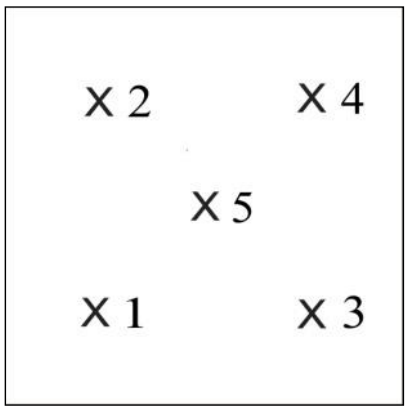

Fig 3: Position of the needle on multi-points to plane configuration

The position of the points that was induced by electric fields was marked with (•) as shown in Figure 4. When viewed from the z-axis, mark (X) and (•) coincides so it is quite marked (X) as shown in Figure 4b. In figure 4 there is point *A(0,0), A(a,0), A(0,a),* and *A(a/2,a/2)* with the horizontal distance $z = c - a$, where *c* is the distance the needle tip to the electrode field.

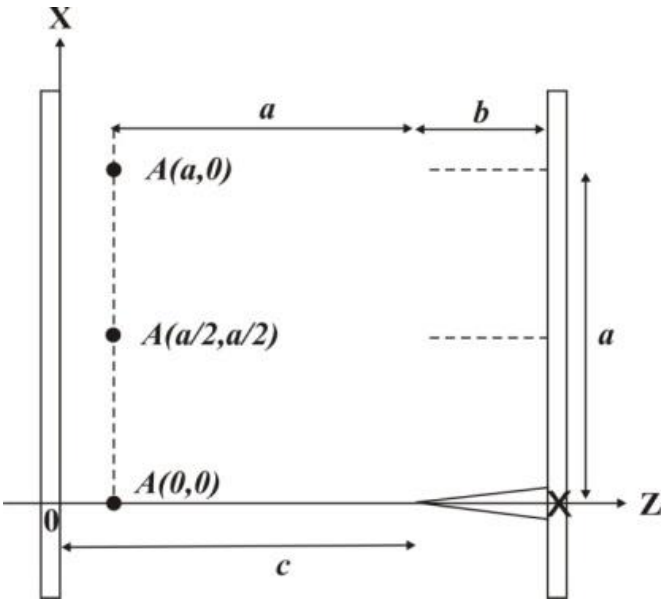

(a)

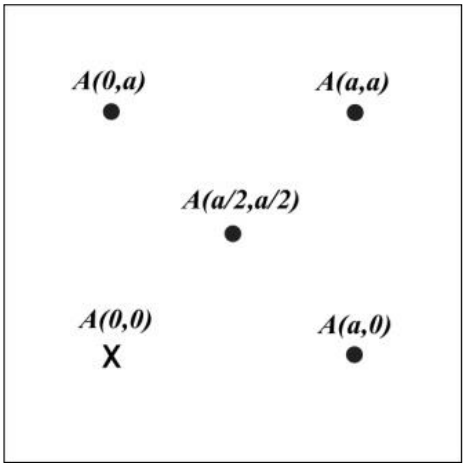

(b)

Fig 4: representation of induced points position on the multi-points to plane configuration with (a) representation of the position of point A (0,0), A(*a*, 0), and A(*a*/2, *a*/2) in the plane XZ and (b) the representation of the position of point A(0,0), A(*a*,0), A(0,a), A(*a*,*a*) and A(*a*/2,*a*/2) in the XY plane when seen from the Z axis

By using equation (9) the electric field generated by a needle electrode at *A(0,0)* point with the position of the axis $x = y = 0$ and $z = c - a$ is

$$E(0,0) = \frac{V / \ln\left(\frac{2}{\varepsilon_1}\right)}{\sqrt{c^2 \cos^4 \zeta + x^2 + y^2}} = \frac{cV / \ln\left(\frac{2}{\varepsilon_1}\right)}{ca - a^2} \tag{21}$$

For the position of other points, namely point A(a, 0), A(0, a), and A(a/2, a/2) induced electric field of a needle in position 1 can be obtained the data in the table 1.

Table 1: The values of *x*, *y*, *u*, and *U* in points I, II, III, IV, V in Figure 5

Point	x	y	z	$u=c^2-\left(x^2+y^2+z^2\right)$	$U=2c^2\cos^2\zeta$ $=u+\sqrt{u^2+4c^2\left(x^2+y^2\right)}$
$A(0,0)$	0	0	$c-a$	$ca-a^2$	$2\left(ca-a^2\right)$
$A(a,0)$	a	0	$c-a$	$ca-2a^2$	$\left(ca-2a^2\right)+\sqrt{\left(ca-2a^2\right)^2+4a^2c^2}$
$A(a,a)$	a	a	$c-a$	$ca-3a^2$	$\left(ca-3a^2\right)+\sqrt{\left(ca-3a^2\right)^2+8a^2c^2}$
$A\left(\frac{a}{2},\frac{a}{2}\right)$	$\frac{a}{2}$	$\frac{a}{2}$	$c-a$	$ca-\frac{3}{2}a^2$	$\left(ca-\frac{3}{2}a^2\right)+\sqrt{\left(ca-\frac{3}{2}a^2\right)^2+2a^2c^2}$

Using the data in Table 1 and the formulation (9) obtained values of the electric field for each point as follows

$$E(0,0)=\frac{cV/\ln\left(\frac{2}{\varepsilon_1}\right)}{ca-a^2} \tag{22}$$

$$E(a,0)=\frac{2cV/\ln\left(\frac{2}{\varepsilon_1}\right)}{\sqrt{\left[U(a,0)\right]^2+4a^2c^2}} \tag{23}$$

$$E(a,a)=\frac{2cV/\ln\left(\frac{2}{\varepsilon_1}\right)}{\sqrt{\left[U(a,a)\right]^2+8a^2c^2}} \tag{24}$$

$$E\left(\frac{a}{2},\frac{a}{2}\right)=\frac{2cV/\ln\left(\frac{2}{\varepsilon_1}\right)}{\sqrt{\left[U\left(\frac{a}{2},\frac{a}{2}\right)\right]^2+2a^2c^2}} \tag{25}$$

To calculate the value of the electric field at a point under the needle, we need to review in advance the needles which affect the value of the electric field at that point. According to Nur et al [12], the maximum value of the ion wind direction angle is 67°. Ion wind direction angle can be determined using arc tan $\theta=\frac{r}{z_1}$, where $r=\sqrt{{x_1}^2+{y_1}^2}$.

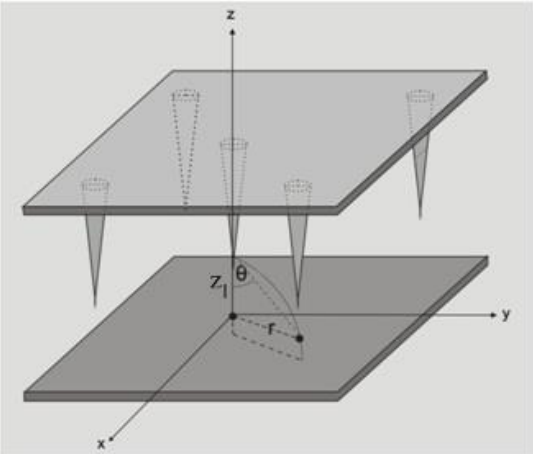

Fig 5: Ion wind direction angle of needle-plane configuration

Ion wind direction angle value for each point and the needle can be seen in Table 2 and 3. Point II, III, and IV whose position is similar to point I have the same ion wind direction angle. The results of these tables show that all ion wind direction angles are not exceeds from 67° so that it can be concluded that all the needles affect the value of the electric field at any point.

Table 2: Ion wind direction angle for point I

Jarum	$r = \sqrt{x_1^2 + y_1^2}$	z_1	$\theta = \tan^{-1}\frac{r}{z_1}$
2	a	A	45°
3	a	A	45°
4	$a\sqrt{2}$	A	54°
5	$\frac{a}{2}\sqrt{2}$	A	35°

Table 3: Ion wind direction angle for point V

Needle	$r = \sqrt{x_1^2 + y_1^2}$	z_1	$\theta = \tan^{-1}\frac{r}{z_1}$
1	$\frac{a}{2}\sqrt{2}$	a	35°
2	$\frac{a}{2}\sqrt{2}$	a	35°
3	$\frac{a}{2}\sqrt{2}$	a	35°
4	$\frac{a}{2}\sqrt{2}$	a	35°

Calculation of the total electric field induces a point done by using the concept of superposition vectors generated from each needle. In general, individual electric field generated a needle can be obtained using the equation

$$\mathbf{E}(x,y,z) = E(x,y,z)\frac{\left\{x_N\mathbf{a}_x + y_N\mathbf{a}_y + z_N\mathbf{a}_z\right\}}{\sqrt{x_N{}^2 + y_N{}^2 + z_N{}^2}}, \quad (26)$$

Where x_N, y_N, and z_N = -a, are a three-dimensional vector length of the needle tip to a specific point position between the needle and plane.

Total electric field which induces a point can be obtained from the superposition of the electric field vector of the five individual needle using equation

$$\mathbf{E}_N = \sum_{\mu=1}^{5}\mathbf{E}_\mu(x,y,z), \quad N = I, II, III, IV, V \quad (27)$$

For example, to calculate the electric field at the position of point I, it can determine in advance the electric field contributed by each needle. When calculating the electric field of a needle, straight point at a distance from the tip of the needle is position $A\ (x, y) = A\ (0.0)$. As shown in Figure 6a to obtain the electric field of the needle 1, then the position of the point I considered a position $A\ (0.0)$ so that the needle 1 donated electric field of $E\ (0.0)$ with $x_N = y_N = 0$. As for obtaining field electricity from the needle 3 as shown in Figure 6b, the position of the point I considered a position $A\ (-a, 0)$ so that the needle 3 donated by the electric field $E\ (-a, 0)$ with x_N = -a, $y_N = 0$ and. For other needles used the same approach with a needle 1 and 3.

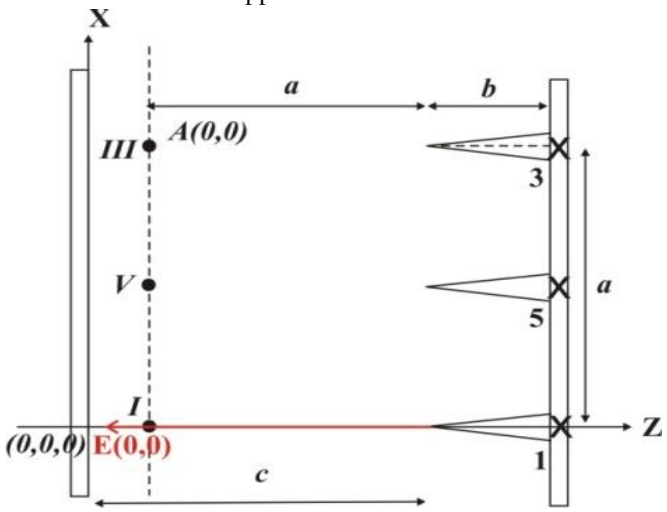

(a)

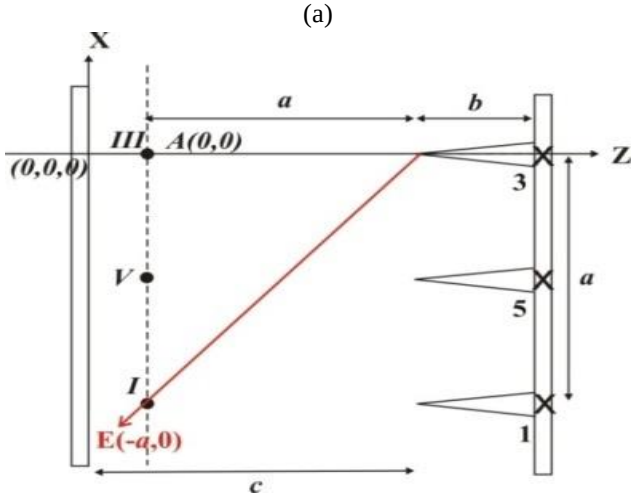

(b)

Fig 6: Representation of the position of point A (a) when calculating the electric field of the needle 1 and (b) when calculating the electric field of the needle 3

By using equation (27), total electric field that induces point I is written as

$$\mathbf{E}_I = -\left[E(0,0)\right]_1 \mathbf{a}_z + \left[E(0,-a)\right]_2 \frac{\left\{-a\mathbf{a}_y - a\mathbf{a}_z\right\}}{\sqrt{2a^2}} + \left[E(-a,0)\right]_3 \frac{\left\{-a\mathbf{a}_x - a\mathbf{a}_z\right\}}{\sqrt{2a^2}}$$
$$+\left[E(-a,-a)\right]_4 \frac{\left\{-a\mathbf{a}_x - a\mathbf{a}_y - a\mathbf{a}_z\right\}}{\sqrt{3a^2}} + \left[E\left(-\frac{a}{2},-\frac{a}{2}\right)\right]_5 \frac{\left\{-\frac{a}{2}\mathbf{a}_x - \frac{a}{2}\mathbf{a}_y - a\mathbf{a}_z\right\}}{\sqrt{\frac{3}{2}a^2}} \quad (28)$$

For N = II, III, IV,dan V

$$\mathbf{E}_{II} = -\left[E(0,0)\right]_2 \mathbf{a}_z + \left[E(0,a)\right]_1 \frac{\left\{a\mathbf{a}_y - a\mathbf{a}_z\right\}}{\sqrt{2a^2}} + \left[E(-a,0)\right]_4 \frac{\left\{-a\mathbf{a}_x - a\mathbf{a}_z\right\}}{\sqrt{2a^2}}$$
$$+\left[E(-a,a)\right]_3 \frac{\left\{-a\mathbf{a}_x + a\mathbf{a}_y - a\mathbf{a}_z\right\}}{\sqrt{3a^2}} + \left[E\left(-\frac{a}{2},\frac{a}{2}\right)\right]_5 \frac{\left\{-\frac{a}{2}\mathbf{a}_x + \frac{a}{2}\mathbf{a}_y - a\mathbf{a}_z\right\}}{\sqrt{\frac{3}{2}a^2}} \quad (28)$$

$$\mathbf{E}_{III} = -\left[E(0,0)\right]_3 \mathbf{a}_z + \left[E(0,-a)\right]_4 \frac{\left\{-a\mathbf{a}_y - a\mathbf{a}_z\right\}}{\sqrt{2a^2}} + \left[E(a,0)\right]_1 \frac{\left\{a\mathbf{a}_x - a\mathbf{a}_z\right\}}{\sqrt{2a^2}}$$
$$+\left[E(a,-a)\right]_2 \frac{\left\{a\mathbf{a}_x - a\mathbf{a}_y - a\mathbf{a}_z\right\}}{\sqrt{3a^2}} + \left[E\left(\frac{a}{2},-\frac{a}{2}\right)\right]_5 \frac{\left\{\frac{a}{2}\mathbf{a}_x - \frac{a}{2}\mathbf{a}_y - a\mathbf{a}_z\right\}}{\sqrt{\frac{3}{2}a^2}} \quad (29)$$

$$\mathbf{E}_{IV} = -\left[E(0,0)\right]_4 \mathbf{a}_z + \left[E(0,a)\right]_3 \frac{\left\{a\mathbf{a}_y - a\mathbf{a}_z\right\}}{\sqrt{2a^2}} + \left[E(a,0)\right]_2 \frac{\left\{a\mathbf{a}_x - a\mathbf{a}_z\right\}}{\sqrt{2a^2}}$$
$$+\left[E(a,a)\right]_1 \frac{\left\{a\mathbf{a}_x + a\mathbf{a}_y - a\mathbf{a}_z\right\}}{\sqrt{3a^2}} + \left[E\left(\frac{a}{2},\frac{a}{2}\right)\right]_5 \frac{\left\{\frac{a}{2}\mathbf{a}_x + \frac{a}{2}\mathbf{a}_y - \mathbf{a}a_z\right\}}{\sqrt{\frac{3}{2}a^2}} \quad (30)$$

$$\mathbf{E}_V = -\left[E(0,0)\right]_5 \mathbf{a}_z + \left[E\left(\frac{a}{2},\frac{a}{2}\right)\right]_1 \frac{\left\{\frac{a}{2}\mathbf{a}_x + \frac{a}{2}\mathbf{a}_y - a\mathbf{a}_z\right\}}{\sqrt{\frac{3}{2}a^2}}$$
$$+\left[E\left(\frac{a}{2},-\frac{a}{2}\right)\right]_2 \frac{\left\{\frac{a}{2}\mathbf{a}_x - \frac{a}{2}\mathbf{a}_y - a\mathbf{a}_z\right\}}{\sqrt{\frac{3}{2}a^2}} + \left[E\left(-\frac{a}{2},\frac{a}{2}\right)\right]_3 \frac{\left\{-\frac{a}{2}\mathbf{a}_x + \frac{a}{2}\mathbf{a}_y - a\mathbf{a}_z\right\}}{\sqrt{\frac{3}{2}a^2}}$$
$$+\left[E\left(-\frac{a}{2},-\frac{a}{2}\right)\right]_4 \frac{\left\{-\frac{a}{2}\mathbf{a}_x - \frac{a}{2}\mathbf{a}_y - a\mathbf{a}_z\right\}}{\sqrt{\frac{3}{2}a^2}} \quad (31)$$

The results of these calculations show that the electric field generated plasma generator multi-points to plane configuration varies at various points around the electrode (not uniform) and the largest electric field contained in point V.

To obtain total electric field of the configuration of multi-points to plane then do superposition electric field of each point in order to obtain total electric field as follows.

$$\begin{aligned}\mathbf{E}_{Total} &= \mathbf{E}_I + \mathbf{E}_{II} + \mathbf{E}_{III} + \mathbf{E}_{IV} + \mathbf{E}_V \\ &= -\left\{5\left[E(0,0)\right] + 8\frac{\left[E(a,0)\right]}{\sqrt{2}} + 4\frac{\left[E(a,a)\right]}{\sqrt{3}} + 8\frac{\left[E\left(\frac{a}{2},\frac{a}{2}\right)\right]}{\sqrt{\frac{3}{2}}}\right\}\mathbf{a}_z \\ &= -\left\{\begin{array}{l} 5\left[\dfrac{cV/\ln\left(\dfrac{2}{\varepsilon_1}\right)}{ca-a^2}\right] + \dfrac{8}{\sqrt{2}}\left[\dfrac{2cV/\ln\left(\dfrac{2}{\varepsilon_1}\right)}{\sqrt{\left[U(a,0)\right]^2+4a^2c^2}}\right] \\ + \dfrac{4}{\sqrt{3}}\left[\dfrac{2cV/\ln\left(\dfrac{2}{\varepsilon_1}\right)}{\sqrt{\left[U(a,a)\right]^2+8a^2c^2}}\right] + \dfrac{8}{\sqrt{3/2}}\left[\dfrac{2cV/\ln\left(\dfrac{2}{\varepsilon_1}\right)}{\sqrt{\left[U\left(\frac{a}{2},\frac{a}{2}\right)\right]^2+2a^2c^2}}\right] \end{array}\right\}\mathbf{a}_z \end{aligned} \tag{32}$$

where

$$U(x,y) = u(x,y) + \sqrt{\left[u(x,y)\right]^2 + 4c^2\left(x^2+y^2\right)}, \tag{33}$$

$$u(x,y) = c^2 - \left(x^2+y^2+z^2\right). \tag{34}$$

The electric field superposition results showed that the total electric field components x and y axis cancel each other out so that the total electric field is simply directed the z axis. This is due to the symmetry of the electric field vector.

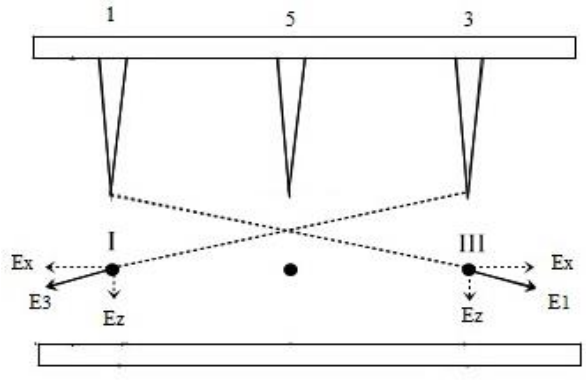

Fig 7: The electric field vector multi-points to plane configuration

For example on the point I, the electric field originating from the needle 3 has a superposition of the electric field vector direction to the x-axis and z-axis. On the point III, the electric field originating from the needle 1 has a superposition of the electric field vector direction to the -x axis and z-axis. When added together, the vector on the x axis will cancel out. This also applies to the needle 5 at the center.

To determine the relationship of the input voltage with an electrical field, equation (32) can be displayed in graphical form an electric field to the input voltage. Assuming the value of $a = 0.01$ m, $c = 0.02$ m, and $\varepsilon 1 = 0.087$, the obtained graph as in Figure 8. From the graph, the form of a linear graph shows that the electric field generated is directly proportional to the input voltage, the greater the input voltage, the electric field generated greater.

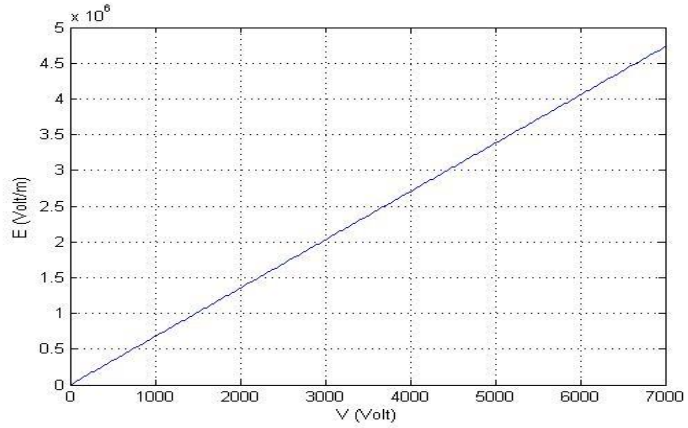

Fig 8: The relationship between the input voltage and the electric field for multi-points to plane configuration

5.2 Current Density of Multi-Points to Plane Configuration

Saturated current in the corona plasma generator with multi-points to plane configuration can be seen with the current density calculation using equation (19). Because total electric field from the calculation is only in z-axis direction, the equation used

$$\mathbf{j} = \mu\varepsilon\left(\nabla \bullet \mathbf{E}\right)\mathbf{E} = \mu\varepsilon\left(\frac{\partial E_z}{\partial z}\right)\mathbf{E} \tag{38}$$

Using the above equation, we obtained the current density for multi-points to plane configuration as written in equation

$$\mathbf{j} = \mu\varepsilon\left\{\begin{array}{l} 5\left[\dfrac{2zcV/\ln\left(\frac{2}{\varepsilon_1}\right)}{\left(c^2-z^2\right)^2}\right] + \dfrac{8}{\sqrt{2}}\left[\dfrac{\left[4zcV/\ln\left(\frac{2}{\varepsilon_1}\right)\right]\left[U(a,0)\right]}{\left(\left[U(a,0)\right]^2+4a^2c^2\right)^{\frac{3}{2}}}\left[1+\dfrac{u(a,0)}{\sqrt{\left[u(a,0)\right]^2+4a^2c^2}}\right]\right] \\ +\dfrac{4}{\sqrt{3}}\left[\dfrac{\left[4zcV/\ln\left(\frac{2}{\varepsilon_1}\right)\right]\left[U(a,a)\right]}{\left(\left[U(a,a)\right]^2+8a^2c^2\right)^{\frac{3}{2}}}\left[1+\dfrac{u(a,a)}{\sqrt{\left[u(a,a)\right]^2+8a^2c^2}}\right]\right] \\ +\dfrac{8}{\sqrt{3/2}}\left[\dfrac{\left[4zcV/\ln\left(\frac{2}{\varepsilon_1}\right)\right]\left[U\left(\frac{a}{2},\frac{a}{2}\right)\right]}{\left(\left[U\left(\frac{a}{2},\frac{a}{2}\right)\right]^2+2a^2c^2\right)^{\frac{3}{2}}}\left[1+\dfrac{u\left(\frac{a}{2},\frac{a}{2}\right)}{\sqrt{\left[u\left(\frac{a}{2},\frac{a}{2}\right)\right]^2+2a^2c^2}}\right]\right] \end{array}\right\} \otimes$$

$$\otimes\left[-\left\{\begin{array}{l} 5\left[\dfrac{cV/\ln\left(\frac{2}{\varepsilon_1}\right)}{c^2-z^2}\right]+\dfrac{8}{\sqrt{2}}\left[\dfrac{2cV/\ln\left(\frac{2}{\varepsilon_1}\right)}{\sqrt{\left[U(a,0)\right]^2+4a^2c^2}}\right] \\ +\dfrac{4}{\sqrt{3}}\left[\dfrac{2cV/\ln\left(\frac{2}{\varepsilon_1}\right)}{\sqrt{\left[U(a,a)\right]^2+8a^2c^2}}\right]+\dfrac{8}{\sqrt{3/2}}\left[\dfrac{2cV/\ln\left(\frac{2}{\varepsilon_1}\right)}{\sqrt{\left[U\left(\frac{a}{2},\frac{a}{2}\right)\right]^2+2a^2c^2}}\right] \end{array}\right\}\mathbf{a}_z\right] \tag{39}$$

where $z = c - a$. the result of the calculation shows that the current density plasma corona generator multi-points to plane configuration resulted saturated currents caused by the shape of the electrodes are not symmetrical.

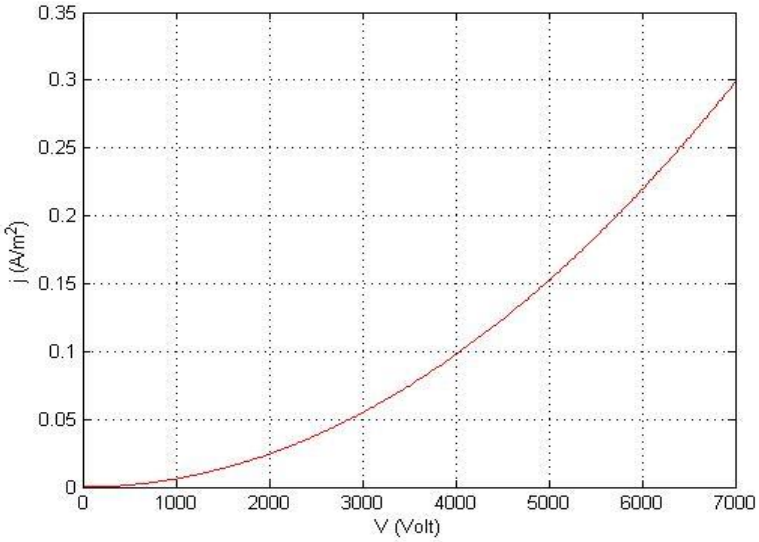

Fig 9: The relationship between current density and voltage input to the plasma generator with a multi-points to plane configuration

6. Experimental validation

To determine the relationship of the input voltage with the current density, equation (39) can be displayed in graphical form the current density of the input voltage. By using the value of the permittivity of air $\varepsilon = 8{,}85 \times 10^{-12}$F / m, the mobility of ions to nitrogen $\mu = 8 \times 10^{-5}$m^2 / Vs [12], a = 0.01 m, c = 0.02 m, and ε1 = 0.087, the obtained graph as in Figure 10. From the figure 9 What appeared parabola graph showing the magnitude of the current density is proportional to the square of the input voltage.

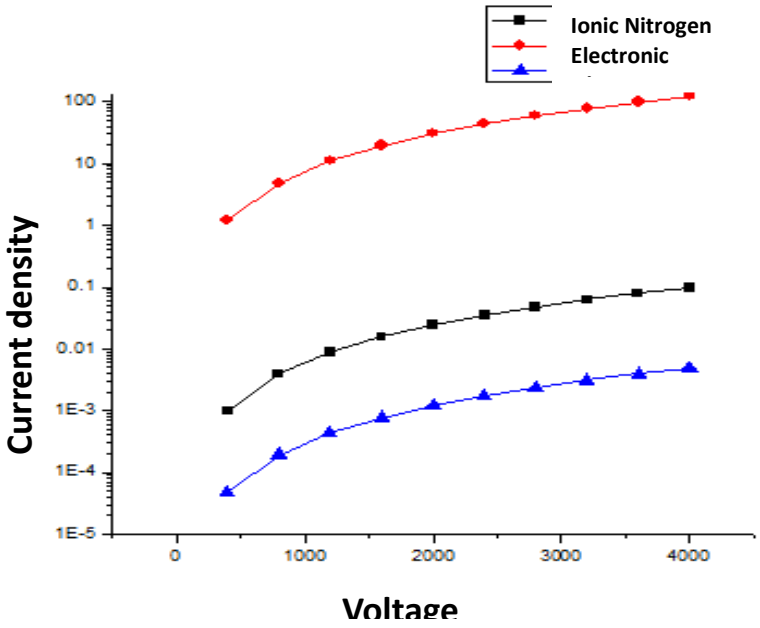

Fig 10: The comparison of the value of the current density on the electronic plasma nitrogen, nitrogen ionic and ionic oxygen

In addition to the form factor of the electrode, the current density of the resulting multi-points to plane configuration are also affected by the magnitude of the charge carrier mobility of the particles. Figure 10 shows a comparison of the value of the current density of the electronic plasma nitrogen, nitrogen ionic and ionic oxygen with nitrogen values for the ionic mobility $\mu = 8 \times 10^{-5}$ m^2 / Vs [12], electronic mobility for nitrogen $\mu = 10^{-1}$ m^2 / Vs [12], and for oxygen ionic mobility $\mu = 3{,}95 \times 10^{-6}$ m^2 / Vs [12]. From the graph shows that the greatest current density on the electronic plasma nitrogen as the greatest mobility value. While the value of the smallest current density in plasma ionic mobility of oxygen due to the smallest value. Figure 11a show the current characteristics as a function of the voltage of the positive corona discharge (CD). In the Figure 11a, it can be seen that the current is a quadratic function (second order polynomial) of the voltage, this is in accordance with the research conducted by Sigmond in 1982 which stated that the current-to-voltage characteristics follow the second-order polynomial equation for corona discharge under atmospheric conditions [15]. It can also be shown that the current as a function of voltage follow law quadratic corona discharge, with a current value proportional to the square of the voltage ($I \approx V^2$)[13,14,16].

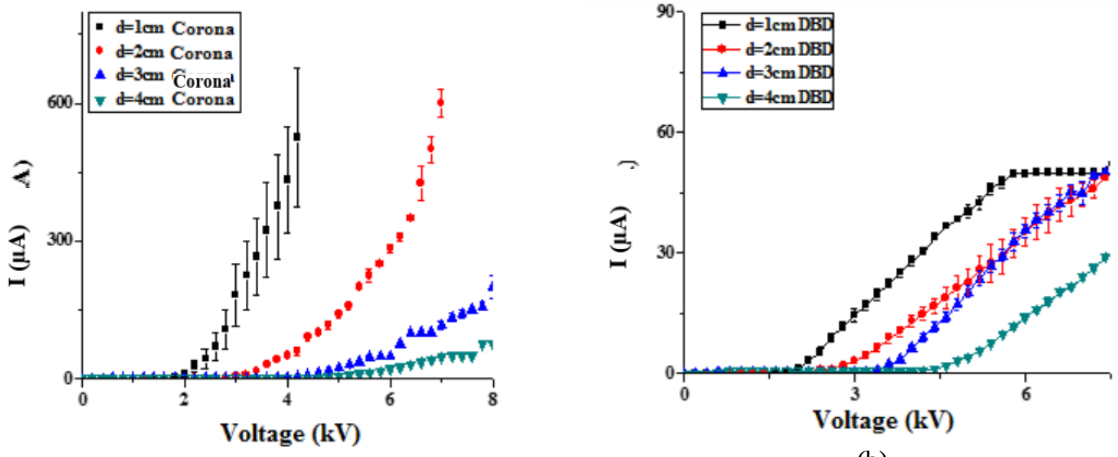

(a) (b)

Fig 11: I-V Characteristics of corona discharge (CD) with multipoint-to-plane configuration (a), and dielectric barrier corona discharge (DBCD) with multipoint-to-plane configuration (b).

According to Sigmond 1982 [15], ions flowing through the charge flow area will produce a current called corona unipolar saturation current. One type of charge carrier unipolar, with mobility μ flows with charge density ρ (r, t) and the current density j = ρv without experiencing diffusion in the electric field E (r, t), the change in charge density (ρ) along the flow:

$$\frac{d\rho}{dt} = \frac{\partial \rho}{\partial t} + \nu . \nabla \rho \qquad (40)$$

By integrating and assuming unipolar ions exist without the influence of space charge with ion flow time (T), then equation 40 becomes,

$$\rho_s = \frac{\varepsilon_0}{\mu T} \qquad (41)$$

with ρ_s called the unipolar ion saturation current density.
If the ion flow distance (d) is in an electric field (E), the flow time T = d/μE can be obtained. It is known that the average ion flow speed ν = μE = μV/h. And ρ_s can be re-expressed as $\rho_s = \varepsilon_0 E/h$, so that the saturation current density is obtained [15].

$$j_s = \rho_s . \mu E = \frac{\mu \varepsilon_0 E^2}{h} \qquad (42)$$

We can show that the current density follows equation (43) for single point to plant

(43)

$$j_s = \frac{\mu \varepsilon_0 V^2}{h^3}$$

Equation (43) is referred to as the corona unipolar saturation current density. The total corona current is proportional to the central current density that spreads twice the square of the point-plane distance which can be written as follows

$$I_s = 2h^2 j \quad (44)$$

By substituting equation (4 3) into equation (44) we will obtain the point-plane corona unipolar saturation current

$$I_s = \frac{2\mu \varepsilon_0 V^2}{h} \quad (45)$$

where I_s represents the unipolar corona saturation current, V represents the corona voltage, μ represents the unipolar ion mobility, ε_0 represents the permittivity of vacuum, h represents the distance between electrodes [15] . The value of this unipolar ion mobility can be calculated using equation (45). But for the case of the multi-point electrode, this equation can be necessary modified a factor of the number of electrode points, which is considered N. In addition, the dielectric constant values also should be corrected. Ffor Dielectric Barrier Corona Discharge (DBCD), we have to use constant of dielectric barrier between two electrodes these barrier can be considered as a dielectric material. Thus, the above equation becomes:

$$I_s = \frac{2\mu \varepsilon_t N V^2}{h} \quad (46)$$

Where ε_t represents the permittivity total material between two electrode. From equation 46, a linear curve s I as a function of V can be made, in order to obtain the gradient of the curve linearity. From the gradient value may be determined and average mobility of the charge carriers in the corona discharge. The effective of dielectric constant between two electrodes should be calculated. From the graphs shown in Figure 11a and Figure 11b, we can see that the unipolar current concept and calculations developed in the paper are very well applicable to corona discharge (CD) but are not suitable for Dielectric Barrier Corona Discharge (DBCD). This is made possible by the effect of an electric dipole in the dielectric material placed on the plant electrode. Discussing the influence of dielectric materials can be an interesting study.

7. Conclusion

From the result of the calculation of electric field and current density generated by plasma generator with multi points to plane configuration, we obtained formulation electric field and current density in the z-axis direction because of the symmetry of the electric field vector in the direction of the x-axis and y. The highest electric field is located on each end of the needle [8] while the electric field at *a* distance from each end of the needle has the largest value in the position of a point under the needle in the middle. The unipolar current concept and calculations developed in the paper are very well applicable to corona discharge (CD) but are not suitable for Dielectric Barrier Corona Discharge (DBCD).Current density value is affected by charge carrier mobility (μ).

Acknowledgements

This research was supported by Universitas Diponegoro, Indonesia, through the RPI (No. 569-126/UN7.D2/PP/V/2023). Authors would like to acknowledge the supports given by research assistants of Centre for Plasma Research, Diponegoro University

References

[1] Köritzer J 2014 Biophysical Effects of Cold Atmospheric Plasma on Glial Tumor Cells (Switzerland: Springer International Publishing)
[2] Jürgen Meichsner Martin Schmidt Ralf Schneider Hans-Erich Wagner (editor) 2013, *Nonthermal Plasma Chemistry and Physics*, Taylor & Francis Group
[3] Siavashani V S, Valipour P and Haghighat E 2014 Fibers Polym 15 729 .
[4] Spyrout, N., Peruos, R., dan Hield, B. (1994) *New Result on a Point–to- Plane DC Plasma Reactor in Low-Pressure Dried Air*, Journal Phys. D: Appl. Phys., Vol. 27, 2329-2339.

[5] Guerra-Garcia, C., Fontanes, P., Urbani, M., Montanya, J., Theodore Mouratidis, Manuel Martinez-Sanchez and Nguyen, N., C., Controlled electric charging of an aircraft in flight using corona discharge, American Institute of Aeronautics and Astronautics, Inc., AIAA Scitech 2020 Forum pp 1-10

[6] Guerra-Garcia, C., Nguyen, N. C., Peraire, J., and Martinez-Sanchez, M., *"Charge control strategy for aircraft-triggered lightning strike risk reduction,"* AIAA Journal, Vol. 56, No. 5, 2018, pp. 1988–2002

[7] Sumariyah Sumariyah, Fauziah Rahmi, Rianti Warto Utami, Asep Yoyo Wardaya, K. Sofyan Firdausi, Fajar Arianto, Zaenul Muhlisin, Sulistiyani Hayu Pratiwi, Heri Sugiarto, Muhammad Nur, (2023), *The mobility of Nitrogen Ions in the Atmospheric Corona Plasma and Its Possibility to Accelerate the Growth of Mung Bean Plants* Journal of Harbin Engineering University Vol. 44 No. 10, pp. 653 - 660

[8] Coelho, R., dan Debeau, J. (1971) *Properties of the Tip – Plane Configuration*, J. Phys. D: Appl. Phys., Vol. 4, 1266-1280.

[9] Wardaya,A.Y., Muhlisin,Z., Hudi, A., Jatmiko Endro Suseno, J.E., Nur, M., Kinandana, A.W., and Jaka Windarta, J., (2020) Eur. Phys. J. Appl. Phys. Volume 89, Number 3, March 2020

[10] Wardaya,A.Y., Muhlisin,Z., Suseno, J.E., Nur, Triadiyaksa, P., Khumaeni, A., Hadi, S., Sarwoko, E.A., and Jaka Windarta (2022), *The Current-Voltage Characteristics for Electrode Geometry Model of Positive DC Corona Discharge in Air*, Gazi University Journal of Science, 35(3): 1140-1150

[11] Nur, M., Azzulkha, A. H., Restiwijaya, M., Muchlisin, Z., dan Sumariyah (2014) *The Study of Electrohydrodynamic and Wind Ions Direction Produced by Positive Corona Plasma Discharge*, Advance in Physics Theories and Applications, Vol. 30, 55-64.

[12] Nur, M. (1997) *Etude des decharges couronne dans l'argan et l'azote tres purs: transport des charges, spectroscopie et influence de la densite*, PhD Thesis, Joseph Fourier University, Grenoble, France

[13] Nur, M., Fadhilah, A., Suseno, A., dan Sutanto, H. (2012) *Mobilitas Ion-ion Ar^+, OH^-, H^+, CO_2, O_2 dan Laju Aliran Angin Ion dalam Plasma Korona pada Tekanan Atmosfer*, Jurnal Mat Stat, Vol. 12 (2), 165-175

[14] Shadrina, N., Susan,A. I., Sasmita, E.,Yulianto, E. ,Restiwijaya, M., Kinandana, A.W., , Pratiwi, S.H., Arianto, F., and Nur, M.,(2019), *Characterization of electrical property and ion mobility in positive corona and dielectric barrier discharge with point to plane configuration*, IOP Conf. Series: Journal of Physics: Conf. Series 1170 012022

[15] Sigmond, R.S., (1982) *Simple approximate treatment of unipolar spacecharge-dominated coronas: the Warburg law and the saturation current*, J. Appl. Phys. 53 pp. 891–898.

[16] Sumariyah, S., Zain,A.Z., Rahmawati, A., Muhlisin, Z., Fajar Arianto, (2022), *Multipoint-Plane Corona Discharge Configuration in Air Analysis and Its Possibility for Accelerating the Growth of Rice*, International Journal of Innovative Science and Research Technology, Volume 7, Issue 6, pp. 232-237